Thermally induced magnetization switching in Gd/Fe multilayers

XU, C., OSTLER, Thomas <http://orcid.org/0000-0002-1328-1839> and CHANTRELL, R. W.

Thermally induced magnetization switching in Gd/Fe multilayers

C. Xu,[1,2,*] T. A. Ostler,[2,3] and R. W. Chantrell[2,†]
[1]*College of Electronic Engineering, South China Agricultural University, Guangzhou, China*
[2]*Department of Physics, University of York, York, YO10 5DD, United Kingdom*
[3]*College of Engineering, Mathematics and Physical Science, University of Exeter, North Park Road, Exeter, EX4 4QF, United Kingdom*
(Received 24 July 2015; revised manuscript received 26 January 2016; published 12 February 2016)

A theoretical model of Gd/Fe multilayers is constructed using the atomistic spin dynamics formalism. By varying the thicknesses and number of layers we have shown that a strong dependence of the energy required for thermally induced magnetization switching (TIMS) is present; with a larger number of interfaces, lower energy is required. The results of the layer resolved dynamics show that the reversal process of the multilayered structures, similar to that of a GdFeCo alloy, is driven by the antiferromagnetic interaction between the transition-metal and rare-earth components. Finally, while the presence of the interface drives the reversal process, we show here that the switching process does not initiate at the surface but from the layers furthest from it, a departure from the alloy behavior which expands the classes of material types exhibiting TIMS.

DOI: 10.1103/PhysRevB.93.054302

I. INTRODUCTION

The question of how magnetization can be reversed is a topic of great practical interest for the manipulation and storage of magnetic information [1]. It is generally accepted that magnetization reversal should be driven by a symmetry-breaking stimulus, for example, by a magnetic field, spin-transfer torque [2], or spin-polarized electric current. In general, the fastest conventional way to reverse magnetization is based on a precessional motion under an orthogonal external magnetic field. A realistic switching time, which can be achieved in such a process, is about 100 ps and is determined by the strength and duration of the magnetic-field pulse [3]. However, it has been discovered that reduction of the magnetic-field pulse durations below about 2–3 ps may result in stochastic magnetization switching [4]. One of the most intriguing alternatives to magnetic-field-induced magnetization switching is making use of a subpicosecond laser pulse [5–8]. Since the first observation of subpicosecond demagnetization of a Ni film subjected to a 60-fs laser pulse, it has been shown that such a pulse is able to cause ultrafast changes in the magnetic state [9]. Subsequently, a femtosecond (fs) laser-induced subpicosecond magnetization reversal across the magnetization compensation temperature (point below the Curie temperature where the magnetization of two sublattices of a ferrimagnet are equal and opposite and sum to zero) was observed in GdFeCo amorphous film [5,10]. Almost at the same time, it has been demonstrated that a sequence of 40-fs circularly polarized pulses can reverse the magnetization without applying external magnetic field in a ferrimagnetic GdFeCo film [6].

Very recently, ultrafast thermally induced magnetization switching (TIMS) [8] has been observed and received wide attention because of its potential application in magnetic recording and optical interconnects [11]. This switching process occurs when an applied subpicosecond heat pulse causes the magnetic state to reverse without any external or implicit magnetic field or circularly polarized light. Several experiments and theoretical descriptions of the underlying physical mechanism have been proposed [8,12–15]. They suggest that the fs heating of the GdFeCo film induces the transient ferromagnetic-like state (TFMLS) [7] and express the switching as an exchange of angular momentum between magnetic sublattices, driven by antiferromagnetic (AFM) exchange coupling. Up to now observations of TIMS are only reported for a narrow composition range of the amorphous rare-earth (RE)–transition-metal (TM) ferrimagnetic alloy film of GdFeCo and TbCo. However, an obvious barrier to technological applications is the use of large amorphous structures, as the key magnetic properties are not scalable to high density. To address this issue, the use of multilayered system has been posed as one solution as it allows for greater control of the structure [16,17]. Therefore, in order to optimize the switching characteristics of TIMS in multilayered systems, we have constructed a theoretical model of Gd/Fe multilayers and performed the comprehensive study of the static and dynamic magnetic properties.

The structure of our paper is as follows: in Sec. II, we introduce the theoretical model of Gd/Fe multilayers constructed by using the atomistic spin dynamics formalism. In Sec. III, we first introduce the structural properties of the Gd/Fe multilayers. After that, we use the atomistic spin dynamics formalism to investigate the static magnetic properties for a range of layer thicknesses and the number of repeats of the layers. The results presented here include the temperature-dependent magnetization curves, which show a decreasing Curie temperature of Fe sublattice and an increasing Curie temperature of Gd sublattice with increasing number of the repeats of the layers. In Sec. IV, we investigate the dynamic magnetic properties focusing on ultrafast TIMS dynamics, the laser energy dependence of switching time of each sublattice, and the layer-resolved magnetization dynamics. Our results show that TIMS in Gd/Fe multilayers occurs in a similar manner as in the GdFeCo alloy, although it requires a minimum number of interfaces. The minimum switching fluence, switching time, and the duration of the TFMLS are strongly dependent on the structural properties, such as the number of repeats of the layers, even though the overall composition of our samples remains constant.

*chudong.xu@york.ac.uk
†roy.chantrell@york.ac.uk

II. ATOMISTIC SPIN DYNAMICS MODEL OF GD/FE MULTILAYERS

The model used in the present work is based on a semiclassical spin model described in detail in Ref. [18] and is outlined briefly here. The system is viewed on an atomistic scale, with each atom having an associated magnetic moment. The basis of the model is the numerical solution of a set of coupled Landau-Lifshitz-Gilbert (LLG) equations of motion for the magnetic moments in an effective field. The effective field combines the deterministic Hamiltonian part and a thermal noise contribution. Each magnetic moment is normalized, such that $\mathbf{S_i} = \boldsymbol{\mu}_i/|\mu_i|$, where μ_i is the magnitude of the magnetic moment at site i. The spin moments are of constant magnitude, allowing no fluctuations in the magnitude of the localized magnetic moment, though the orientation can take any position on a sphere.

We use the Heisenberg form of the exchange for nearest neighbours to describe the energetics of the system by the following Hamiltonian:

$$\mathcal{H} = -\sum_{i \neq j} J_{ij}\, \mathbf{S}_i \cdot \mathbf{S}_j - \sum_i d_z\, \mathbf{S}_{i,z}^2, \tag{1}$$

where J_{ij} is the exchange integral between spins i and j (i, j are lattice sites), $\mathbf{S}_i$ is the normalized vector, and d_z is the uniaxial anisotropy constant (assumed along z). It is important to note here the significance of the sign of J_{ij}. For ferromagnetic (FM) materials, where neighboring spins align in parallel, $J_{ij} > 0$, and for antiferromagnetic materials, where the spins prefer to align antiparallel, $J_{ij} < 0$. Here we assume that the exchange constants do not vary with a change in the structure, allowing us to study the structural effects systematically. This approximation also allows us to make a direct comparison with the alloy [19].

We model the magnetization dynamics of the system via the use of the LLG equation [20], given by

$$\frac{\partial \mathbf{S}_i}{\partial t} = -\frac{\gamma_i}{\left(1+\lambda_i^2\right)\mu_i}\mathbf{S}_i \times \left(\mathbf{H}_{\text{eff}}^i + \lambda_i\, \mathbf{S}_i \times \mathbf{H}_{\text{eff}}^i\right). \tag{2}$$

Here λ_i and γ_i are the Gilbert damping parameter and the gyromagnetic ratio, respectively, with effective field $\mathbf{H}_{\text{eff}}^i$:

$$\mathbf{H}_{\text{eff}^i} = -\frac{\partial \mathcal{H}_i}{\partial \mathbf{S}_i} + \boldsymbol{\zeta}_i. \tag{3}$$

Here $\boldsymbol{\zeta}_i$ represents a stochastic term, which describes the coupling to the external heat bath. The thermal fluctuations are included as a white-noise term, uncorrelated in time, which is added into the effective field. This form of the noise is treated as a Stratonovich stochastic process [21]. The correlators of different components of this field can be written as

$$\langle \zeta_{i,a}(t) \rangle = 0, \tag{4}$$

$$\langle \zeta_{i,a}(t)\zeta_{j,b}(t') \rangle = \frac{2\mu_i k_{\text{B}}}{\gamma_i}\lambda_i T \delta_{ij}\delta_{ab}\delta(t-t'), \tag{5}$$

where a,b refer to the Cartesian components of the spin vector and i,j to separate spins (i.e., uncorrelated spatially). T is the temperature of the heat bath to which the spin is coupled. The coupling of the spins to the heat bath (λ_i) is a parameter which attempts to describe all of the energy and momentum transfer channels into and out of the spin system, for example, from the lattice and conduction electrons. Note that there is a subtle difference between a local microscopic damping parameter λ_i and a macroscopic damping parameter, as measured for a material in an experiment, usually denoted as α [22], the Gilbert damping. Although the intrinsic damping is also known to be temperature dependent [23], this intrinsic temperature dependence, naturally included in the atomistic approach, is normally ignored in the modeling of magnetization dynamics [24,25].

It should be noted that since we have two different species, there are some subtleties with regard to the implementation of the model due to the presence of onsite parameters that enter into the LLG equation. Such onsite parameters include λ_i, μ_i, and γ_i, as well as three types of exchange interactions $J_{\text{Fe-Fe}}$, $J_{\text{Gd-Gd}}$, and $J_{\text{Gd-Fe}}$. Experimentally there is a difference in the effective gyromagnetic ratio of each species due to inhomogeneities in the crystal-field potential [26]. The effect of different gyromagnetic ratios gives rise to the existence of the temperature at which the ratio $\mathrm{M}_1/\gamma_1 - \mathrm{M}_2/\gamma_2$ goes to zero, known as the angular momentum compensation temperature T_A. At T_A there is no angular momentum associated with the magnetization, which can thus be moved by the slightest torque [26]. For simplicity, we have assumed that each sublattice has the same gyromagnetic ratio of $1.76 \times 10^{11}\ T^{-1}\ \mathrm{s}^{-1}$, which is the free electron value. In our simulation, we assume that the Fe and Gd coupling to be $\lambda_{\text{Fe}} = \lambda_{\text{Gd}} = 0.01$, which is the same with the Ref. [8].

III. STRUCTURAL PROPERTIES AND STATIC MAGNETIC PROPERTIES

In this section, we first introduce the Gd/Fe multilayered structure parameters and the related simulation parameters. Then we use the atomistic spin dynamics formalism to investigate the static magnetic properties for a different number of repeats of the layers.

A. Structural properties

The samples studied here are Gd/Fe multilayers, which have a fixed composition (75% Fe and 25% Gd) for the entire system and a fixed lateral dimensions and height. The aim then is to investigate the effect of the number of layers on the switching properties precluding composition effects. The structure is shown schematically in Fig. 1, where we have used the symbol N to indicate the number of repeats of the layer. Furthermore, we use $L_{Fe} = x$, where x represents the number of Fe unit cell layers in each repeat structure, and use $L_{Gd} = y$ to describe the number of Gd unit cell layers. For instance, $N = 1$ is a bilayer structure consisting of 96 unit cell layers of Fe ($L_{Fe} = 96$) and 32 of Gd ($L_{Gd} = 32$). $N = 2$ has 2 repeats, each consisting of 48 unit cell layers of Fe ($L_{Fe} = 48$) and 16 of Gd ($L_{Gd} = 16$) up to $N = 32$, which has 32 repeats, each consisting of 3 unit cell layers (6 planes) of Fe and 1 unit cell layer (2 plane) of Gd. In our model, we use a face-centered cubic (fcc) unit cell, so each unit cell layer contains two atomic planes. Due to a reduced translational invariance of multilayered films, we expect different magnetization dynamics for Fe (Gd) planes lying a given distance from an interface with Gd (Fe). This will

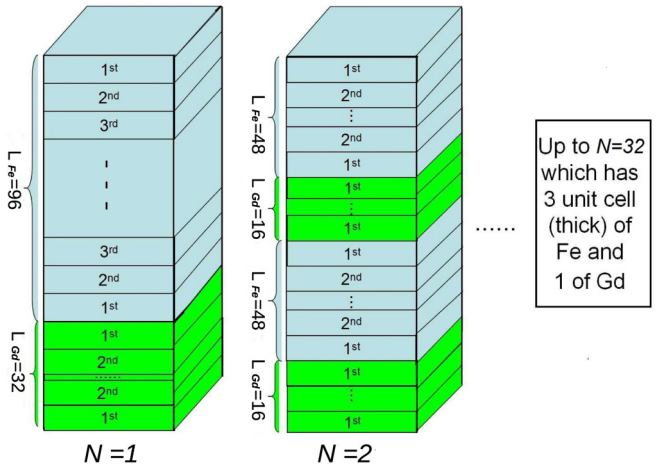

FIG. 1. Schematic of the Gd/Fe multilayered structures.

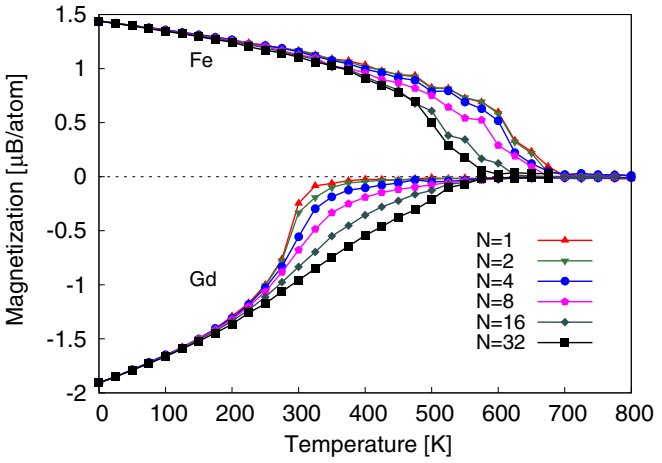

FIG. 2. Numerically calculated magnetization curves of each sublattice for the Gd/Fe mulitlayers as a function of temperature. Results are shown for a range of the number of repeats of the layers.

be shown and discussed later in greater detail. To describe the dependence of antiferromagnetic coupling on the distance to the Gd-Fe interface, it is necessary to distinguish the location of each atomic plane, as shown in Fig. 1. We use 1st, 2nd, 3rd, and so on to describe the nearest, the second nearest, the third nearest atomic plane, and so on to the Gd-Fe interface. Due to the periodic structure, for each Fe repeat structure or Gd repeat structure, it has two Gd-Fe interface (upper interface and bottom interface) and we use two 1st atomic planes to present the planes nearest to the upper interface and the bottom interface, respectively. And this rule also applies to the second nearest (2nd) and third nearest (3rd) atomic planes, and so on.

It should be noted that for synthetic multilayers to exhibit TIMS it is essential to consider the physical requirements of the structure analogous to those of intrinsic RE-TM ferrimagnets. The first property is the antiferromagnetic exchange coupling of the component layers of the synthetic ferrimagnet [8]. The second criterion is the existence of distinct magnetization dynamics for the two component layers, which allows the formation of a transient ferromagnetic state and drives the switching process [7]. So, in our system, the Fe layers are antiferromagnetically coupled to the Gd layers. The exchange values $J_{\text{Fe-Fe}} = 2.835 \times 10^{-21}$ J, $J_{\text{Gd-Gd}} = 1.26 \times 10^{-21}$ J, and $J_{\text{Gd-Fe}} = -1.09 \times 10^{-21}$ J are derived for the alloy and parameterized from experimental observation. This factor is potentially important in relation to ultrafast magnetization processes, because the intersublattice exchange could provide a mechanism for energy transfer from the Fe to Gd [19]. Since the uniaxial component of the magnetocrystalline anisotropy is dominant in the composition range where the compensation point occurs, therefore in our model we assume a uniaxial anisotropy energy of 8.07246×10^{-24} J per atom. This value should be strong enough to support perpendicular magnetization in the multilayers.

B. Temperature-dependent magnetization

In the following we present calculations of the static magnetic properties of Gd/Fe multilayers by using the constructed atomistic spin model. We first simulate the temperature-dependent magnetization, as shown in Fig. 2. These results were obtained by simulating a system of $32 \times 32 \times 128$ fcc unit cells (524 288 spins) with periodic boundary conditions. For each of the Fe and Gd spins we write a Landau-Lifshitz-Gilbert equation and solve it using the Heun numerical integration scheme [27–30]. The system is equilibrated until there is only a small change in the magnetization for each temperature point. In our simulation, we choose the value of $\mu_{\text{Fe}} = 1.92\mu_B$ as an effective magnetic moment for the Fe sublattice, where μ_B is the Bohr magneton. For the Gd sites, we use the bulk value of $\mu_{\text{Gd}} = 7.63\mu_B$ [31]. It should be noted here that the value of 1.92 for Fe is an effective magnetic moment containing the contribution of Fe and Co. Actually, the small amount of Co (9.3%) is added experimentally to support the perpendicular anisotropy as in $Gd_{25}Fe_{65.7}Co_{9.3}$ alloy. For simplicity, we choose TM sublattice as an FeCo sublattice, since the amount of it is small and both Fe and Co are coupled ferromagnetically. This same simplification has been used in a number of previous works [7,8,15]. Furthermore, the use of the perpendicular anisotropy is not necessary for the reversal of the magnetization. In-plane magnetization will still undergo TIMS as long as the Gd and Fe sublattices are antiferromagnetically coupled [8].

As shown in Fig. 2, when the number of repeats of the layers is increased, the Curie temperature of Fe gradually decreases while that of Gd gradually increases. According to the previous report [19], the temperature dependence of the magnetization of each sublattice will be different depending on the effective exchange. For GdFeCo ferrimagnetic alloys, there exists a polarization effect of the TM (FeCo) sublattice on the RE(Gd) sublattice due to the antiferromagnetic exchange coupling. This polarization effect also changes the temperature dependence of the magnetization. Our results indicate that the polarization effect strengthens with the rise in the number of repeats. It is obvious that the effect of increasing the number of repeats of the layers strengthens the antiferromagnetic exchange coupling as the number of Gd-Fe surfaces increases. Consequently, the Fe sublattice and the Gd sublattice tend to share a common Curie temperature due to the increased

coupling between the Fe sublattices and Gd sublattices. When the number of repeats reaches 32, i.e., sample $N = 32$, it forms a common Curie temperature about 550 K, consistent with the alloy.

So far we have shown that the effect of the number of repeats in the structure modulates the antiferromagnetic exchange interaction and has a great impact on the static magnetic properties of Gd/Fe multilayers. By changing the number of repeats in the structure the Curie temperature of each sublattice can be adjusted. Based on these results, it is natural to raise some questions accordingly. First, how will the modulation of the antiferromagnetic interaction by the number of repeats influence the dynamic magnetic properties? Second, do Gd/Fe multilayers have a similar magnetic dynamics to a GdFeCo alloy? Most important, can TIMS be obtained in multilayers as in the alloy? In the next section, these questions will be analyzed and answered in greater detail.

IV. DYNAMIC MAGNETIC PROPERTIES

Atomistic spin models have been used previously for the study of short time-scale dynamics [32] excited by fs laser pulses in ferromagnets and ferrimagnets, giving good agreement with experimental time scales for the ultrafast magnetization dynamic process [7,8]. In this section, we use this model to investigate dynamic magnetic properties of Gd/Fe multilayers.

To simulate the effect of fs laser excitation, we have employed the two-temperature model [33] to model the electron and phonon heat baths to which the spin system may couple. The two-temperature model describes the change in the temperature of the electron and phonon baths under the action of a laser pulse. The temperature dynamics are governed by two coupled differential equations:

$$C_e(T_e)\frac{dT_e}{dt} = -G_{el}(T_l - T_e) + P(t), \tag{6}$$

$$C_l\frac{dT_l}{dt} = -G_{el}(T_e - T_l). \tag{7}$$

In the equations $P(t)$ is the time-dependent laser power, which is related to the pump fluence P_0 by the equation $P(t) = P_0 \exp\{-[(t-\tau_p)/\tau_p]^2\}$ (here, τ_p is the pump time of the laser). The electron-phonon coupling factor G_{el} and the lattice specific-heat capacity C_l are taken to be independent of temperature [7,8,15]. In our work we assume that the electronic temperature, T_e, is coupled to the magnetic system through the correlator Eq. (5). A previous report [34] shows that the electron-coupling factor is reduced by the excitation of d-band electrons but this occurs at high temperatures and so this effect should be minimal in the situations considered here. The parameters used were [7,8,15] $G_{el} = 1.7 \times 10^{18}$ J m^{-3} K^{-1} s^{-1}, $C_l = 3 \times 10^6$ J m^{-3} K^{-1}, and $C_e(T_e) = \gamma_e T_e$, where γ_e is the electronic specific-heat constant [35] and $\gamma_e = 2.25 \times 10^2$ J m^{-3} K^{-2}. Note that the value of γ_e used here is more appropriate to Fe alloys and is similar to the value used by Mendil *et al.* [36]. Using these parameters the relevant time scale of the lattice temperature dynamics can be calculated, determined by the electron-phonon coupling time $C_l/G_{el} = 1.765$ ps, which describes the exponential decay of the lattice temperature towards a constant electron temperature after the initial rapid increase. The coupling of Fe and Gd spin systems to the electron system is based on previous studies [32,37] of fast relaxation in transition metals which concluded that only a coupling of the spin to the conduction electrons was sufficient to cause subpicosecond demagnetization, though this remains a debated topic in the literature [38].

In the simulations, the fs laser pulse is chosen as a Gaussian pulse with 50-fs pulse width. We start at an initial temperature of 80 K [7], and the electronic temperature is increased up to a peak temperature before dropping down to the final equilibrium temperature.

In the following, by using the model introduced above, we present the simulation results of the dynamic magnetic properties for Gd/Fe multilayers, including ultrafast TIMS dynamics, switching probability of multilayers, laser energy dependence of switching time, and layer-resolved magnetization switching dynamics. Since the system size is quite large, the statistical error is rather small. Our results indicate a strong dependence on the layer thicknesses, resulting in markedly different dynamics compared to the case of an amorphous alloy.

A. Ultrafast thermally induced magnetization dynamics

First, we study the ultrafast thermally induced magnetization dynamics to determine whether the TIMS can be obtained in multilayers. Based on the results of temperature-dependent magnetization calculations, sample $N = 32$ shows a similar temperature-dependent magnetization to the alloy, with the Fe layer and Gd layer sharing a common Curie temperature. Therefore, it is reasonable for sample $N = 32$ to be our first choice in studying the magnetization dynamics.

Figure 3(a) shows the time dependence of the electron and phonon temperature from the two-temperature model, which demonstrates that the electronic temperature increase rapidly initially, being reduced on the picosecond time scale to be in equilibrium with the phonon temperature. Since the value of the electronic specific heat constant γ_e is smaller than the corresponding value using in Ref. [8] for GdFeCo alloy, a higher electron temperature is observed, which is consistent with Ref. [36]. The magnetization dynamics at short delay time of Fig. 3(b) shows that the ultrafast demagnetization occurs first due to the fast interaction between the spin and the hot electrons described by the two-temperature model. Then the magnetization changes slowly due to slow cooling of the whole system. In this stage, the magnetization can evolve to three different cases, as clearly shown in Fig. 3(c) at the long delay time, which are dependent on the laser energy (the laser energy E is related to the pump fluence P_0 as $E = \sqrt{\pi}\tau_p P_0$). Consider first the case of low energy (0.98 G J/ m^3) excitation; here the magnetization relaxes slowly back towards the initial state on a timescale of a few ps. The cooling of the magnetic system requires thermalization of the phonon bath via energy transfer to the surroundings, which requires around 1 ns. This is much longer than the time scale of our simulations, within which the initial equilibrium state is not reached. The second case is, under the medium energy (1.05 G J/ m^3), the magnetization decreases slowly and then relaxes slowly to the initial state. The last case is, under the high energy (1.12 G J/ m^3), the

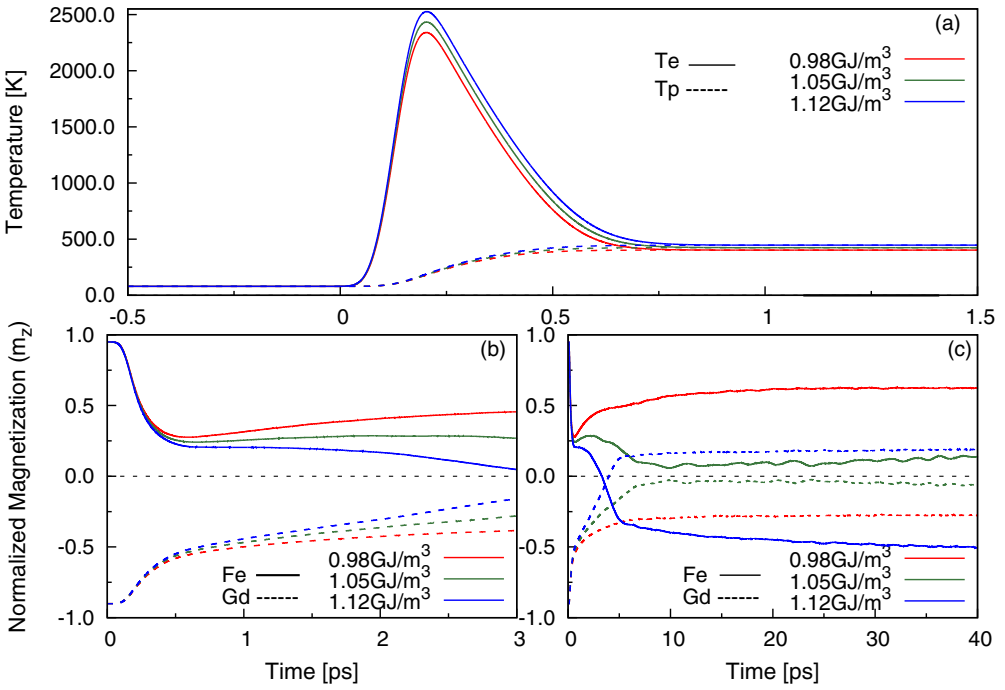

FIG. 3. (a) Time dependence of the electron and phonon temperature from the two-temperature model. (b) and (c) Ultrafast magnetization dynamics curves for the Fe (solid lines) and Gd sublattices (dashed lines) for a range of pump fluences for 32 repeats ($N = 32$) at short delay time in panel (b) and at long delay time in panel (c). Note the three different time scales for the axes in panels (a), (b), and (c).

magnetization reverses slowly to the opposite direction, which shows thermally induced magnetization switching. Also this switching shows the occurrence of the TFMLS in which the two antiferromagnetically coupled Fe and Gd become temporarily aligned.

The results presented here show that this multilayer has a similar pump fluence dependence on the magnetization dynamics to GdFeCo alloys [6]. Furthermore, our results demonstrate that TIMS can be obtained in multilayers though it has been previously demonstrated in bilayers [17].

B. Switching probability of multilayers

As mentioned before, to investigate the possibility of TIMS in other multilayers, we have calculated the fs laser-induced ultrafast magnetization dynamics for all the samples introduced in Sec. II. Our results indicate that a certain minimum number of layers (at least 8 repeats in the structure) is required to switch via TIMS. Since the composition of the samples is fixed, it is the increase of the number of repeats of the layers that leads to the increase of the effective Gd-Fe antiferromagnetic exchange, which is inversely proportional to the layer thickness, resulting in TIMS, consistent with Ref. [15]. The switching arises when a sufficient number of AFM interfaces are present. Our results indicate a minimum number of AFM surface compared the volume is required corresponding to an effective interface exchange energy of approximately -2×10^7 mJ/cm^3.

In order to obtain the switching window for those multilayers, that can switch via TIMS, we further calculate the switching probability following laser pulses of increasing energy, as shown in Fig. 4. The data are obtained by averaging the results from ten statistically independent calculations. The results show that the minimum switching energy decreases with increase of the number of repeats of the layers. Consequently, the strengthening of the antiferromagnetic exchange interaction can decrease the minimum switching energy. Clearly the optimum switching (that is the highest switching probability and the widest energy range) occurs in the sample having the most layers due to the strongest antiferromagnetic exchange interaction. The result can help us to design a new multilayered material which has the optimum TIMS performance.

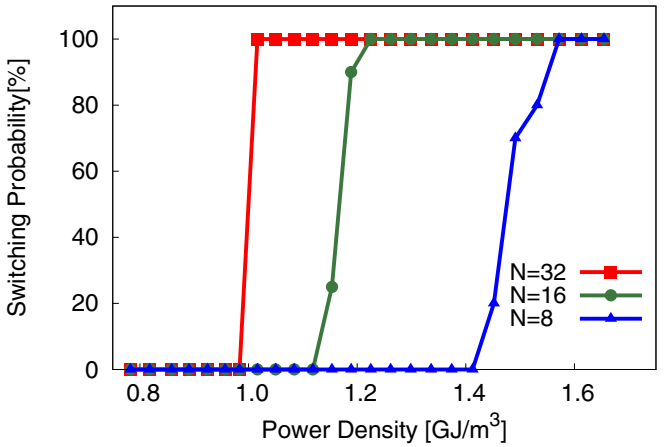

FIG. 4. Numerically calculated the switching probability as a function of the laser energy for samples $N = 8$, $N = 16$, and $N = 32$.

C. Laser energy dependence of switching time

The switching process associated with TIMS, as stated in the introduction, occurs via the TFMLS, as reported in Ref. [7]. It remains an open question as to whether the reversal process in the multilayer structures occurs via the same route. In Ref. [7], the TFMLS was due to the presence of AFM exchange, and therefore in the multilayer system one might expect that the number of AFM interfaces would play a role in the duration of such a nonequilibrium state. Furthermore, as the switching is due to the AFM exchange one would expect the interface layer to reverse first followed by the layers increasingly distant from the interface. With the present model we shed light on this by investigating the layer-resolved dynamics and show that the picture is somewhat more complicated.

First, we calculate the switching time of the Fe sublattice and Gd sublattice respectively as a function of laser energy for the different samples. We then break down the process on a layer-by-layer level. The results of the switching times of the individual sublattices are shown in Fig. 5. For each sample, the switching time of the Fe sublattice decreases monotonically with increase of the laser energy, while that of Gd sublattice varies in a more complicated manner. Specifically, it initially decreases with increase of the laser energy and increases for higher fluence. It is clear from Fig. 5 that the thinner layer as a whole switches on a faster time scale driven by the AFM exchange, which accelerates magnetization dynamics, consistent with Ref. [39]. The nonmonotonic variation of the reversal times of each sublattice with pump fluence is an interesting feature of the reversal processes. Initially, as the pump fluence is increased, the mechanism driving the switching process is more strongly excited, leading to a reduction in the switching times of both sublattices. At higher laser energies more energy is pumped into the system that must be dissipated, leading to an increase in the duration of the transient ferromagnetic-like state duration (difference between upper and lower lines for each structure).

So far we have discussed the properties of the magnetization of each of the Fe and Gd species by averaging over all

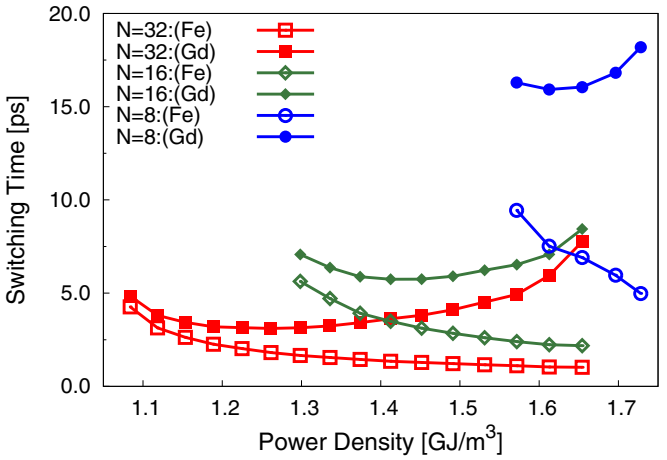

FIG. 5. Switching times of both Fe sublattice and Gd sublattice as a function of the laser energy for samples $N = 8$, $N = 16$, and $N = 32$.

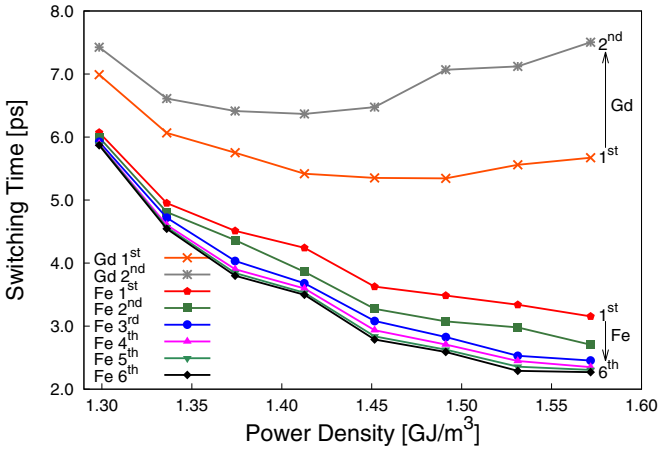

FIG. 6. Layer-resolved reversal times for each Fe and Gd plane in the $N = 16$ structure. The direction of the arrows represent the direction away from the interface to the central plane. The numbers represent the plane index where 1st is the interface plane up to the central plane (2nd for Gd and 6th for Fe).

of the layers. However, in multilayer systems in general there is a lack of translational invariance [40] which creates distinct *environments* for each of the layers with the potential for each layer to have its own dynamics. Investigating the layer-resolved dynamics in such systems is extremely difficult experimentally [40] and it is not immediately obvious how such dynamics contribute to the overall magnetization of each species. In the following we investigate the layer-resolved dynamics of our Gd/Fe system and, in particular, quantify the variations in the switching times of each layers. This gives us more detailed insight into the results of Fig. 5.

The results of the layer-resolved switching time of both the Gd and Fe sublattices of the $N = 16$ system are shown in Fig. 6. The nearest Gd plane (the interface layer) switches first, consistent with the AFM-driven dynamics. However, surprisingly, the Fe layers show the opposite trend with the so-called bulk layers reversing first, with the interface plane reversing last. Our results demonstrate that while the AFM interfaces are essential to drive the reversal, the interface Fe plane is slowed by its interaction with the intrinsically slower Gd species. This is consistent with the explanation of the origin of the switching via the excitation of spin-wave modes [15].

The initiation of the reversal at the Fe planes furthest from the interface is due to the fact that the presence of Gd at the interface *slows* the motion of the Fe plane closest to it. The ultrafast demagnetization of Gd has been shown to be much slower than its transition metal counterparts [38]; however, in the presence of antiferromagnetic exchange coupling, its demagnetization rate is decreased [39]. This is consistent with the results of Fig. 6. However, the Fe behavior is slowed due to the presence of the Gd and quickens as the layers become *bulk*like. This shows that the switching of the multilayer structures is intrinsically linked with the demagnetization times of the layers. Thus, although the Gd/Fe multilayer structures exhibit TIMS, the mechanism is significantly different from that of the alloy, expanding the class of materials supporting the TIMS phenomenon.

V. CONCLUSION

To conclude, we have constructed a theoretical model based on atomic spin dynamics to investigate the laser-induced dynamic properties of Gd/Fe multilayers with different numbers of repeats of the layers and demonstrated the possibility of TIMS in these multilayer structures. Our results show that the Gd-Fe interlayer antiferromagnetic exchange coupling, which has an important impact on the static and dynamic magnetic properties, can also be modulated by using different number of repeats in the structure due to the change of the effective Gd-Fe exchange interaction.

The calculated temperature dependence of the magnetization shows that with the increase of the number of repeats of the layers, the Curie temperature of the Fe sublattice decreases while that of Gd increases due to the strengthened Gd-Fe antiferromagnetic exchange. The simulations of fs laser-induced ultrafast magnetization dynamics show TIMS occurring in Gd/Fe multilayers. The results demonstrate that the dependence of the switching time on the laser energy is qualitatively similar to the amorphous GdFeCo alloys. Furthermore, the switching dynamics is also strongly dependent on the structural properties. The minimum switching energy and the switching time decrease with the increase of the number of repeats of the layers due to the increase of Gd-Fe antiferromagnetic exchange. These results show that the optimum switching occurs in the sample with the most repeats in the structure. However, somewhat surprisingly the switching in the Fe layer is not initiated at the interface but in the bulk consistent with a spin-wave-driven process. Our findings have significant consequences of the development of low-energy-structured materials for TIMS.

ACKNOWLEDGMENTS

The authors would like to acknowledge financial support of the European Commission under Contract No. 281043, FemtoSpin, and the Advanced Storage Technology Consortium. C. Xu also would like to acknowledge support of the National Natural Science Foundation of China (Grant No.61308038), China Scholarship Council (CSC), and Natural Science Foundation of Guangdong China (Grants No. S2013040015235 and No. 2015A030313400).

[1] J. Stohr and H. C. Siegmann, in *Magnetism: From Fundamentals to Nanoscale Dynamics* (Springer, Berlin, 2006).
[2] Z. Li and S. Zhang, Phys. Rev. B **69**, 134416 (2004).
[3] T. Gerrits, H. A. M. van den Berg, J. Hohlfeld, L. Bar, and T. Rasing, Nature (London) **418**, 509 (2002).
[4] I. Tudosa, C. Stamm, A. B. Kashuba, F. King, H. C. Siegmann, J. Stohr, G. Ju, B. Lu, and D. Weller, Nature (London) **428**, 831 (2004).
[5] C. D. Stanciu, A. Tsukamoto, A. V. Kimel, F. Hansteen, A. Kirilyuk, A. Itoh, and Th. Rasing, Phys. Rev. Lett. **99**, 217204 (2007).
[6] C. D. Stanciu, F. Hansteen, A. V. Kimel, A. Kirilyuk, A. Tsukamoto, A. Itoh, and T. Rasing, Phys. Rev. Lett. **99**, 047601 (2007).
[7] I. Radu, K. Vahaplar, C. Stamm, T. Kachel, N. Pontius, H. Dürr, T. A. Ostler, J. Barker, R. F. L. Evans, R. W. Chantrell, A. Tsukamoto, A. Itoh, A. Kirilyuk, T. Rasing, and V. Kimel, Nature (London) **472**, 205 (2011).
[8] T. A. Ostler, J. Barker, R. F. L. Evans, R. W. Chantrell, U. Atxitia, O. Chubykalo-Fesenko, S. El Moussaoui, L. Le Guyader, E. Mengotti, L. J. Heyderman, F. Nolting, A. Tsukamoto, A. Itoh, D. Afanasiev, B. Ivanov, M. Kalashnikova, K. Vahaplar, J. Mentink, A. Kirilyuk, T. Rasing, and V. Kimel, Nat. Commun. **3**, 666 (2012).
[9] E. Beaurepaire, J. C. Merle, A. Daunois, and J. Y. Bigot, Phys. Rev. Lett. **76**, 4250 (1996).
[10] C. Stanciu, A. Kimel, F. Hansteen, A. Tsukamoto, A. Itoh, A. Kirilyuk, and T. Rasing, Phys. Rev. B **73**, 220402(R) (2006).
[11] Z. A. Azim, X. Fong, T. A. Ostler, R. W. Chantrell, and R. Kaushik, IEEE Electron Device Lett. **35**, 1317 (2014).
[12] A. R. Khorsand, M. Savoini, A. Kirilyuk, A. V. Kimel, A. Tsukamoto, A. Itoh, and T. Rasing, Phys. Rev. Lett. **108**, 127205 (2012).
[13] J. Mentink, J. Hellsvik, D. Afanasiev, B. Ivanov, A. Kirilyuk, A. Kimel, O. Eriksson, M. Katsnelson, and T. Rasing, Phys. Rev. Lett. **108**, 057202 (2012).
[14] U. Atxitia, T. Ostler, J. Barker, R. F. L. Evans, R. W. Chantrell, and O. Chubykalo-Fesenko, Phys. Rev. B **87**, 224417 (2013).
[15] J. Barker, U. Atxitia, T. A. Ostler, O. Hovorka, O. Chubykalo-Fesenko, and R. W. Chantrell, Sci. Rep. **3**, 3262 (2013).
[16] S. Mangin, M. Gottwald, C.-H. Lambert, D. Steil, V. Uhlir, L. Pang, M. Hehn, S. Alebrand, M. Cinchetti, G. Malinowski, Y. Fainman, M. Aeschlimann, and E. E. Fullerton, Nat. Mater. **13**, 286 (2014).
[17] R. F. L. Evans, T. A. Ostler, R. W. Chantrell, I. Radu, and T. Rasing, Appl. Phys. Lett. **104**, 082410 (2014).
[18] U. Nowak, in *Handbook of Magnetism and Advanced Magnetic Materials,* Vol. 2 (John Wiley & Sons, Hoboken, NJ, 2007).
[19] T. A. Ostler, R. F. L. Evans, R. W. Chantrell, U. Atxitia, O. Chubykalo-Fesenko, I. Radu, R. Abrudan, F. Radu, A. Tsukamoto, A. Itoh, A. Kirilyuk, T. Rasing, and A. Kimel, Phys. Rev. B **84**, 024407 (2011).
[20] T. L. Gilbert, IEEE Transactions on Magnetics **40**, 3443 (2004).
[21] J. L. García-Palacios and F. J. Lázaro, Phys. Rev. B **58**, 14937 (1998).
[22] O. Chubykalo-Fesenko, U. Nowak, R. W. Chantrell, and D. Garanin, Phys. Rev. B **74**, 094436 (2006).
[23] K. Gilmore, Y. U. Idzerda, and M. D. Stiles, Phys. Rev. Lett. **99**, 027204 (2007).
[24] D. Berkov, in *Handbook of Magnetism and Advanced Magnetic Materials* (Springer, Sussex, 2006).
[25] B. Skubic, J. Hellsvik, L. Nordström, and O. Eriksson, J. Phys. Condens. Matter **20**, 315203 (2008).
[26] R. K. Wangsness, Phys. Rev. **91**, 1085 (1953).
[27] D. Lewis and N. Nigam, J. Comput. Appl. Math. **151**, 141 (2003).

[28] M. Aquino, C. Serpico, and G. Miano, J. Comput. Phys. **209**, 730 (2005).
[29] J. H. Mentink, M. V. Tretyakov, A. Fasolino, M. I. Katsnelson, and T. Rasing, J. Phys. Condens. Matter **22**, 176001 (2010).
[30] R. F. L. Evans, W. J. Fan, P. Chureemart, T. A. Ostler, M. O. A. Ellis, and R. W. Chantrell, J. Phys.: Condens. Matter **26**, 103202 (2014).
[31] J. Jensen and A. R.Mackintosh, in *Rare Earth Magnetism: Structures and Excitations* (University of Copenhagen, Clarendon, UK, 1991).
[32] N. Kazantseva, U. Nowak, R. W. Chantrell, J. Hohlfeld, and A. Rebei, Europhys. Lett. **81**, 27004 (2008).
[33] J. Chen, D. Tzou, and J. Beraun, Int. J. Heat Mass Transf. **49**, 307 (2006).
[34] Z. Lin and L. V. Zhigilei, Appl. Surf. Sci. **253**, 6295 (2007).
[35] R. Chimata, A. Bergman, L. Bergqvist, B. Sanyal, and O. Eriksson, Phys. Rev. Lett. **109**, 157201 (2012).
[36] J. Mendil, P. Nieves, O. Chubykalo-Fesenko, J. Walowski, T. Santos, S. Pisana, and M. Münzenberg, Sci. Rep. **4**, 3980 (2014).
[37] M. Fähnle, J. Seib, and C. Illg, Phys. Rev. B **82**, 144405 (2010).
[38] B. Koopmans, G. Malinowski, F. Dalla Longa, D. Steiauf, M. Fähnle, T. Roth, M. Cinchetti, and M. Aeschlimann, Nat. Mater. **9**, 259 (2010).
[39] I. Radu, C. Stamm, A. Eschenlohr, F. Radu, R. Abrudan, K. Vahaplar, T. Kachel, N. Pontius, R. Mitzner, K. Holldack, A. Fölisch, R. F. L. Evans, T. A. Ostler, J. H. Mentink, R. W. Chantrell, A. Tsukamoto, A. Itoh, A. Kirilyuk, A. V. Kimal, and T. Rasing, SPIN **05**, 1550004 (2015).
[40] K. Zakeri, T. Chuang, A. Ernst, L. M. Sandratskii, P. Buczek, and Y. Zhang, Nat. Nanotechnol. **8**, 853 (2013).